Journal of Environmental Sciences Vol.16, No.3, pp.509—512, 2004

ISSN 1001—0742
CN11—2629/X

Article ID: 1001-0742(2004)03-0509-04 **CLC number:** X513; O407 **Document code:** A

Research on buildings impacting on aerosol diffusing in urban area using remote sensing

YANG Sheng-tian[1], YANG Zhi-feng[1], MAO Xian-qiang[1], ZHU Qi-jiang[2]

(1. Institute of Environment, Beijing Normal University, Beijing 100875, China. E-mail: yangshengtian@263.net; 2. Center for RS & GIS, Beijing Normal University, Beijing 100875, China)

Abstract: Employing remote sensing method to interpret the building volumetric ratio and aerosol status in Guangzhou, China. The relation between them and identified characteristics of their spatial distribution was analyzed. Results showed that building density and aerosol status are strongly correlated. It is indicated that the resistance of building to aerosol diffusing is one of factors influencing air pollution in urban area. On the basis of calculated results, building voluminous ratio of 5.6 is taken as the threshold impacting on aerosol diffusing, so the building voluminous ratio of Guangzhou should be limited to less than 5.6 in order to alleviate air pollution.

Keywords: remote sensing; aerosol; building voluminous ratio; air pollution

Introduction

The aerosol above an area is a major indicator of air pollution. The density and the thickness of aerosol are influenced by either air pollutant discharged from urban or aerosol diffusing feasibility. It is important to study aerosol diffusing while clarifying the processes of air pollutions in urban. Remote sensing has directly obtained some data of the land surface, so it is an effective tool to monitor ecosystem (Alex, 2002; Ni, 1999; Zhang, 2001). With the satellite being improved and the techniques of remote sensing application being developed, the remotely sensed data has been used to solve some ecological problems on urban scale (Wang, 1999). Nowadays, we have known many achievements such as using remote sensing to identify water pollution (Chen, 2000) and to design ecological plan in urban area (Wang, 2000; Zeng, 1997; Wang, 1997). Our work is different from these examples. We choose Guangzhou, as a case study, interpret the spatial information of the aerosol and building volumetric ratio (BVR) based on remotely sensed data ETM$^+$ on November 1, 2000, and showed the connections between the aerosol density and BVR. Subsequently, we concluded that the buildings in urban area are resistance to aerosol diffusing.

1 Interpreting aerosol

1.1 The principle

Aerosol is solid or liquid particles floating in air. It reflects and to scatters electromagnetic wave. If the incident atmospheric radiation is ignored, the radiative transfer models may be written in a very simple way:

$$L_s = L_a + \tau_a \times L_g, \quad (1)$$

where L_s is the radiance as measured by satellite, L_a is the radiance reflected and scattered by atmosphere, τ_a is the atmospheric transmittance, and L_g is the ground radiance. Obviously, L_a and τ_a are strongly correlated to aerosol density and thickness, so the radiative transfer model, Eq. (1), can be transferred to the formula relevant to aerosol status:

$$L_s = f(A) \times L_g, \quad (2)$$

where $f(A)$ represents the aerosol function. After atmospheric correction, the atmospheric influence is alleviated to some extent, and then $f(A)$ is reduced to $f'(A)$. Therefore, Eq. (2) is written as:

$$L'_s = f'(A) \times L_g, \quad (3)$$

where L'_s is the radiance measured by satellite after atmospheric correction. Continuously, we define the ratio between band 1 and band 4 of ETM$^+$ before atmospheric correction as L_{un}, and define the ration between band 1 and band 4 after atmospheric correction as L_{cr}, then combining Eqs. (2) and (3), L_{un} and L_{cr} are given as follows:

$$L_{un} = \frac{f(A_1) \times L_{g1}}{f(A_4) \times L_{g4}} = f(\nabla_A) \times \frac{L_{g1}}{L_{g4}}, \quad (4)$$

$$L_{cr} = \frac{f'(A_1) \times L_{g1}}{f'(A_4) \times L_{g4}} = f'(\nabla_A) \times \frac{L_{g1}}{L_{g4}}, \quad (5)$$

where the suffix 1 and 4 respectively refer to band 1 and band 4. Consequently, the diverge ΔL between L_{un} and L_{cr} is given below:

$$\Delta L = L_{un} - L_{cr} = [f(\nabla_A) - f'(\nabla)] \times \frac{L_{g1}}{L_{g4}} = \Delta f(\nabla_A) \times \frac{L_{g1}}{L_{g4}}. \quad (6)$$

It is known that the pixel radiances within the same type of land surface are close. We can use the ratio between two bands to reduce the radiative difference among pixels. As result, in Eq. (6), we can assume the L_{g1}/L_{g4} is similar within one type of land surface. Finally, we define aerosol index as:

$$L_{index} = \frac{\Delta L}{\Delta L_{st}}, \quad (7)$$

in the Eq. (7), L_{index} presents Aerosol Index, ΔL presents diverge between L_{un} and L_{cr} in the region where there is aerosol, and ΔL_{st} presents diverge between L_{un} and L_{cr} in the

standard region that take as clear atmosphere reference. Thus, according to Eq. (6), Eq. (7) is transferred to the formula:

$$L_{\text{index}} = \frac{\Delta f(\nabla_A)}{\Delta f_{\text{st}}(\nabla_A)} \times \lambda, \quad (8)$$

$$\lambda = \left(\frac{L_{\text{gl}}}{L_{\text{g4}}}\right) \Big/ \left(\frac{L_{\text{gl,st}}}{L_{\text{g4,st}}}\right), \quad (9)$$

in the two equations above, the suffix st means the variables are for the standard region. In this paper, our task is to research urban buildings resisting effect to aerosol diffusing, so we assume land surface properties are similar in urban area. Therefore, in Eq. (8), λ is close to 1 and L_{index} is mainly determined by $\Delta f(\nabla_A)/\Delta f_{\text{st}}(\nabla_A)$. It is reasonably recognized that L_{index} mainly shows the relative difference of aerosol status. Since we require the spatial distribution of relative grades of aerosol in our study rather than precise density or thickness of aerosol, L_{index} is accurate enough to satisfy our application.

1.2 The procedure

The flow chart of interpreting aerosol is shown in Fig.1. The studying steps are: (1) The ETM$^+$ data is divided into two groups. One group is corrected by atmospheric correction method, Dark Substraction (Hao, 1999), and its ratio L_{cr} between band 1 and band 4 is calculated. Another group ratio L_{un} between band 1 and band 4 is also calculated, but not corrected by atmospheric correction. (2) The diverge ΔL between two groups L_{cr} and L_{un} is obtained. (3) Taking clear air as the standard ΔL_{st}, we calculate the aerosol index L_{index}. While calculating the aerosol index L_{index}, we take the clean air above the urban region near Liuxihe Reservoir as standard ΔL_{st}.

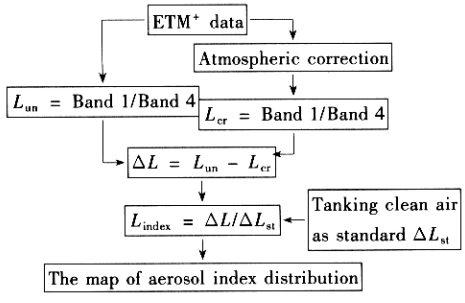

Fig.1 The flow chart of obtaining aerosol

2 Interpreting the urban area

As described in preceding paragraph, interpreting the urban is essential for obtaining aerosol index and making it comparable. The flow chart adopted in our work to distinguish the urban class from other land cover classes is given in Fig.2. Our work steps are: (1) While ETM$^+$ 6 bands (band 1, band 2, band 3, band 4, band 5, band 7) are atmospherically corrected, they are transformed by principle components analysis. The first principle component represents light, and the second principle component represents vegetation and water. (2) Some regions covered by building, water or vegetation, they are chosen to give their statistics. (3) Making use of the these statistics, the model is inferred to interpret all regions covered by building as the first principle component minus the second principle component:

$$P = PC_1 - PC_2 (\text{when } PC_1 - PC_2 > 0), \quad (10)$$

where P is the regions covered by building, PC_1 is the matrix of the first principle component, and PC_2 is the matrix of the second principle component.

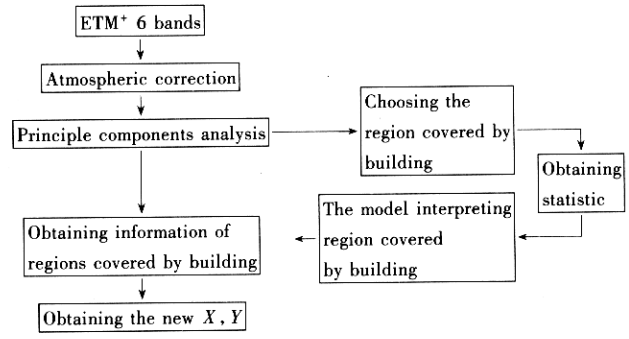

Fig.2 The flow chart of obtaining the land covered by buildings in urban

To summarize, we extracted the urban class from other land cover classes by means of method described above, and took this urban class as the study region. As the consequence, we obtain the spatial distribution of relative aerosol difference in the region of Guangzhou (Fig.3a) by using model (7) addressed in Section 1.

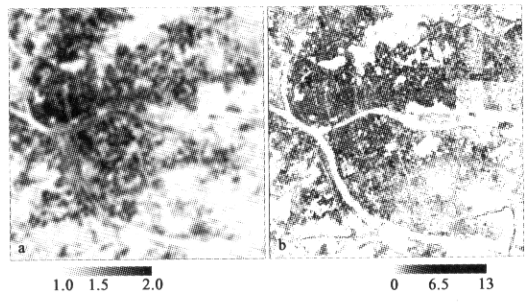

Fig.3 Using remote sensing to obtaining aerosol and *BVR* (part)

3 Interpreting building volumetric ratio

Building volumetric ratio (*BVR*), which represents the number of building in urban, means the total built-up area per spatial unit. We give the model as Eq. (11) to retrieve *BVR* with remotely sensed data.

$$B = \frac{\sum_1^{N'} \frac{H' \times b'^2}{h'}}{S_c}, \quad (11)$$

We assume the building combined with nearby small buildings which we define as Building Unit. So H' in Eq. (11) is the height of building unit, b' is the length of building unit top's side, and N' is the number of building unit. S_c is the area occupied by N' building units, which includes the area of building fundament and the building

accessories. While retrieving N' with remotely sensed data, we regard S_c as a pixel area. Because we utilize ETM$^+$ data in our work and its pixel is 30 m by 30 m, S_c is equal to 900 m^2. After surveying the condition of building in Guangzhou, we determine that H', b' and h' are 10 m, 10 m and 3 m respectively. According to Geometrical-optical model (Research System Inc; Li, 1986; 1992) and boolean regular, N' in Eq. (11) can be transferred as follow equation:

$$\rho_s = e^{-N'\left(\frac{b'^2 + b' \times H' \times \mathrm{tg}\theta}{S_c}\right)} \times \rho_g + \left(\frac{b'^2}{S_c} \times \rho_b + \frac{b' \times H' \times \mathrm{tg}\theta}{S_c} \times \rho_z\right) \times N', \quad (12)$$

where ρ_s is the land surface reflectance, ρ_g is the reflectance of unlighted building surface, ρ_b is the reflectance of lighted building surface, and ρ_z is the reflectance of shadow. All of these parameters can be directly obtained from remotely sensed data. θ is the solar zenith angle deriving from the time of satellite passing Guangzhou.

BVR in Guangzhou was calculated with Eq. (12) and shown in Fig.3b. We check up the *BVR* against Guangzhou digital map(1:10000), the accuration up to 81% means that the result is satisfactory.

4 The analysis of urban building resistance to aerosol diffusing

4.1 The relationship between aerosol and *BVR*

It is easy to understand from Fig. 3 that the spatial distribution of the aerosol and *BVR* is consistent. Besides, Fig.4 presents the condition of aerosol index and *BVR* at the same transect in Guangzhou, from which we can identify that aerosol index is consistent to *BVR*. In order to give how much is the resistance of building density to aerosol diffusing, we calculate the correlation index between aerosol index and *BVR* by:

$$\rho_{x,y} = \frac{\mathrm{Cov}(X, Y)}{\rho_x \times \rho_y}, \quad (13)$$

where

$$-1 \leqslant \rho_{x,y} \leqslant 1$$

and

$$\mathrm{Cov}(X, Y) = \frac{1}{n}\sum_{i=1}^{n}(x_i - \mu_x)(y_i - \mu_y).$$

Where ρ_x, ρ_y are standard deviations, μ_x, μ_y are means, and X, Y is respectively matrix of Aerosol Index and *BVR*. We obtained the correlation index between X and Y by Eq. (13), which is equal to 0.72. We believe that the building density actually influences the aerosol diffusing. The more is the number of buildings, the greater is *BVR*. Higher building density has stronger resistance to air flowing, so the aerosol diffusing is often weaker in the region of greater *BVR*.

4.2 The relationship between aerosol index and *BVR* grade

Dividing the *BVR* in Guangzhou into 5 grades: <2.8, $2.8—5.6$, $5.6—8.4$, $8.4—11.2$ and >11.2, we calculated aerosol index means of every *BVR* grade(Fig.5). From Fig. 5 the relations between aerosol index and *BVR* grades are found: (1) Most pixels whose *BVR* is <2.8 fall in the scope where aerosol index is <1.2, i.e. there is little aerosol. (2) Most pixels whose *BVR* is in 2.8—5.6 fall in the scope where the aerosol index is in 1.2—1.4. This feature showed that the aerosol in urban is enhanced while *BVR* increasing. (3) Most pixels whose *BVR* is >5.6 fall in the scope where the aerosol index is about 1.6. This feature shows the air quantity is still serious. (4) The curves' feature of *BVR* grades: 5.6—8.4, 8.4—11.2 and >11.2, indicated that although the *BVR* grades increase, their scopes of aerosol index do not change, meaning that air quantity does not become more serious. For these reasons, *BVR* equal 5.6 should be regarded as the threshold in which the building in Guangzhou is an obvious resistance to aerosol diffusing.

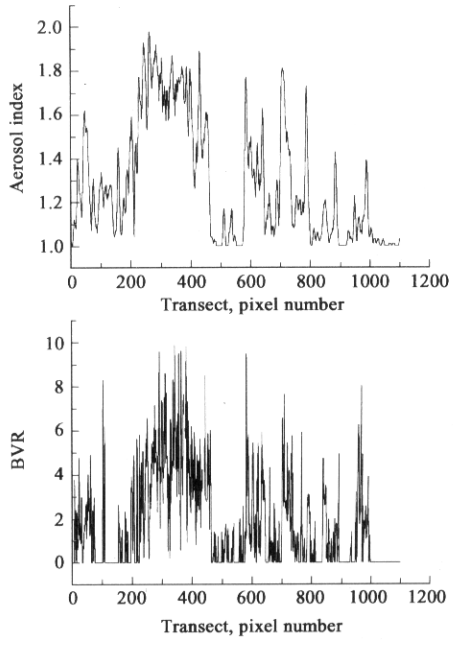

Fig.4 The condition of aerosol index and voluminous ratio of building on the same transverse section

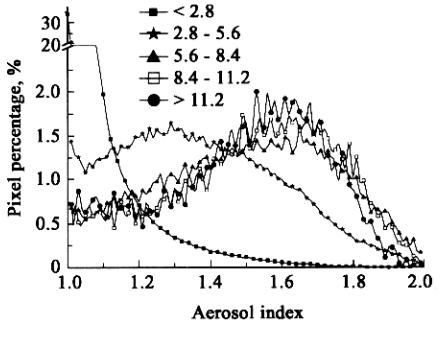

Fig.5 The spatial statistic of aerosol index

5 Conclusions

The air pollution in urban is resulted from human activities. Efforts are usually devoted to pollution sources controlling. However, it is not ignorable that the urban land surface, especially the urban building, is a resistance to aerosol diffusing. After applying remote sensing methods to study the aerosol status and *BVR* in Guangzhou, here are conclusions: (1) The *BVR* in urban and the aerosol status in urban is strongly correlated, it is proved that the buildings density is resistance to aerosol diffusing. (2) *BVR* equal to 5.6 is the threshold in Guangzhou. When *BVR* is lease than 5.6, the building does not affect on aerosol diffusing. When *BVR* is more than 5.6, the building resists aerosol diffusing obviously. Therefore, limiting the build density is helpful to alleviate air pollution.

Although our work has shown that remote sensing is an effectual tool to disclose ecological problems on the urban scale, there are shortages in our work. Relative difference of aerosol is used to analyze the aerosol status and land surface influence is not thoroughly ruled out by the approach of interpreting aerosol. In addition, utilizing ETM^+ data of one time period and lacking of meteorological data of long time series, it is impossible for us to study urban aerosol status by combining meteorological method and remote sensing technology.

Acknowledgement: The authors thank to Pro. He Jian-bang in IGNRR, CAS for providing the remote sensing data.

References:

Alex de Sherbinin, Karen Line, Kal Raustiala, 2002. Remote sensing data: valuable support for environmental treaties[J]. Environment, 44(1): 20—31.

Chen S P, Xie C J, 2000. Urban remote sensing and urban geo-information system[J]. Science of Surveying and Mapping, 25(1): 1—9.

Hao R M, Qin S H, Han X S, 1999. The analysis of situation of landscape ecological envrionment in Huhhot area[J]. Journal of Arid Land Resources and Environment, 13(sup):112—117.

Li X, Strahler A H, 1986. Geometrical-optical bi-directional modeling of a conferous forest canopy, IEEE trans[J]. Geosci. Remote Sensing, GRS-24: 906—919.

Li X, Strahler A H, 1992. Geometrical-optical directional modeling of the discrete-crown vegetation canopy, Effect of croen shape and mutual shadowing, IEEE trans[J]. Geosci Remote Sensing, GRS-30: 276—292.

Ni S X, Jiang J J, Wang J C, 1999. Landscape ecology of the region surrounding Qinghai Lake, Qinghai Province of China based on remote sensing[J]. Journal of Environmental Sciences, 11(2): 211—215.

Research System Inc. ENVI online help navigator[EB]. WWW: http://www.envi-sw.com, http://www. ResearchSystems.com/envi.

Wang J J, Shu J M, Cao J X *et al*., 1997. Monitoring on landscape changes in Sanya[J]. China Environmental Science, 17(3): 233—236.

Wang W J, Zhang J H *et al*., 1999. Introduction to main aspects remote sensing application in environmental and ecological monitoring[J]. Environmental Monitoring in China, 15(6): 48—51.

Wang X J, Ma T, 2000. The application of remote sensing technology in monitoring the water quality of Taihu Lake[J]. Environmental Science, 21(6):65—68.

Zeng H, Guo Q H, Liu J Y, 1997. Analysis of landscape ecological changing characteristics of Dongguan City[J]. China Environmental Science, 17(5): 422—425.

Zhang J H, Fu C B, Hiroshi Kanzawa, 2001. Simulating canopy stomatal conductance of winter wheat and its distribution using remote sensing information[J]. Journal of Environmental Sciences, 13(4): 439—443.

(Received for review March 27, 2003. Accepted May 15, 2003)